Table 9. Statistics of radon-monitoring site and its correlation with meteorological parameters

Parameter	Avg.	Std.dev.	Avg + std	Percentage vari. coefficient (C%) Std./Avg.	Correlation coefficient
Radon (Counts/24 h)	5728	4802	15330	83	–
Evaporation (mm)	2.65	2.53	7.71	95	– 0.08
Temperature (°C)	22.01	12.17	46.35	55	0.10
Relative humidity (%)	47.56	20.19	87.94	42	0.12
Wind velocity (km/h)	5.53	1.76	9.05	32	– 0.14
Rainfall (mm)	40.57	56.38	153.33	138	0.08

it precedes the occurrence of earthquakes. Although the concept of negative peak is there, there is no exact demarcation, from where and to what level the value will decrease. A low or high value in radon emanation may be due to meteorological variations too. The results reveal that radon emanation is directly correlated with temperature, relative humidity and rainfall, and inversely with evaporation and wind velocity (Table 9).

Finally, we may conclude that there is a high microseismic activity in the region and the stations in close proximity of MBT record impulsive values of radon before an impending seismic event. Sensitivity of a radon-monitoring station also depends upon the geological conditions of the region, nature of the soil and the meteorological variations.

1. Birchard, G. F. and Libby, W. F., *J. Geophys. Res.*, 1980, **85**, 3100–3106.
2. King, C. Y., *J. Geophys. Res.*, 1980, **85**, 3065–3078.
3. King, C. Y., *Earthquake Prediction Res.*, 1984, **3**, 13–34.
4. Teng, T., *J. Geophys. Res.*, 1980, **85**, 3989–3099.
5. Teng, T., Sun, L. and Mcraney, J. K., *Geophys. Res. Lett.*, 1981, **8**, 441–444.
6. Hauksson, E. and Goddard, J. G., *J. Geophys. Res.*, 1981, **86**, 7037–7054.
7. Wakita, H., Narkamura, Y., Notsu, K., Noguchi, M. and Asada, T., *Science*, 1980, **207**, 882–883.
8. Virk, H. S. and Singh, B., *Nucl. Geophys.*, 1992, **6**, 287–291.
9. Virk, H. S. and Singh, B., *Tectonophysics.*, 1993, **227**, 215–224.
10. Ulomov, V. I. and Mavashev, B. Z., *Dokl. Akad. Sci. USSR Earth Sci. Sect.*, 1967, **176**, 9–11.
11. Virk, H. S., *Nucl. Geophys.*, 1995, **9**, 141–146.
12. Wedpohl, K. H., *Handbook of Geochemistry*, Springer, Berlin, 1978.
13. Virk, H. S., Walia, V. and Sharma, A. K., *Curr. Sci.*, 1995, **69**, 452–454.
14. Thorsteinsson, T., Proceedings of 2nd U.N. Symposium on Development and use of Geothermal Resources, US Govt. Printing Office, Washington DC, 1973, pp. 2173–2180.
15. Andrews, J. N., Proceedings of 2nd International Symposium on Water-Rock Interaction, 1977, pp. 334–342.
16. Dobrovolsky, I. P., Zubkov, S. I. and Miachkin, V. I., *Pure Appl. Geophys.*, 1979, **117**, 1025–1044.
17. Anderson, O. L. and Grew, P. C., *Rev. Geophys. Space Phys.*, 1977, **15**, 77–104.
18. King, C. Y., *Nature*, 1978, **271**, 516–519.

ACKNOWLEDGEMENTS. We thank DST, New Delhi for financial support. We are grateful to Dr V. P. Kamble, Director Seismology, IMD, New Delhi for supplying the microseismic data of the region for correlation purposes.

Received 30 July 1996; revised accepted 17 March 1997

A feasibility study towards absolute dating of Indo-Gangetic alluvium using thermoluminescence and infrared-stimulated luminescence techniques

M. Someshwar Rao, B. K. Bisaria* and A. K. Singhvi

Physical Research Laboratory, Navarangpura, Ahmedabad 380 009, India

*Geological Survey of India (NR), Lucknow 226 024, India

Results of a successful maiden attempt to date the Indo-Gangetic alluvium using the luminescence dating technique are presented. The low equivalent dose for the surface sample indicates that these samples had experienced a solar resetting of geologically acquired luminescence. The infrared stimulated luminescence ages on other terraces range from ~ 2 to 15 ka and are stratigraphically consistent.

THE 0.25 million sq km Gangetic plain is a foreland basin, extending from Delhi ridge in the west to Rajmahal hills in the east and from Siwaliks in the north to Bundelkhand–Vindhyan high-lands in the south. Major rivers on this plain, viz. Ganga, Yamuna, Ramganga, Ghaghra, Gandak, etc. originate in the Himalaya and carry a large sediment load towards Bay of Bengal. The alluvial fill shows a south-eastward decrease in thickness[1] and this varies from 1000 m in the north near Himalaya to < 10 m in the south adjoining peninsular shield. The basement of the Ganga basin is segmented by a number of transversely occurring geofractures, giving a horst and graben topography[2]. This structural fabric of the basin was responsible for the creation of a number of sub-basins such as the Western UP Shelf, Faizabad

Ridge, Eastern UP Shelf, etc. Evidences indicate that during Quaternary, reactivation of these geofractures resulted in the neotectonic adjustments, leading to a relative sinking and uplifting of the different blocks as manifested by morphologic changes of rivers such as meander cut-off, straightening of course and migration of confluence. This scenario suggests that the alluviation dynamics was controlled by them. Table 1 provides a summary of the lithostratigraphy of the Ganga plain in UP[3-5].

The Gangetic plain of UP is a thick pile of Quaternary sediments overlying a northerly slopping basement[2,6], comprising rocks of Bundelkhand gniessic complex (BGC), Delhi Group, Vindhyan Group and Siwalik Group. The Quaternary alluvium for which the dating has been attempted, has been classified into Older Alluvium comprising Banda and Varanasi Alluvial deposits. The New Alluvium consists of fan deposits near the foothills of Himalaya and, terrace and recent alluvial deposits within the valley fills of present day rivers.

The flood plain restricted to the present day valley of the rivers has been classified into older flood plain, comprising erosional terrace, depositional terrace (T_1) and active flood plain (T_0) representing present day meander belt of the rivers[7]. These aggradational surfaces are of regional character and possess a Holocene top soil[8]. These structures have been suggested to be formed as a result of variation in the gradient of river streams in response to eustatic sea level changes[9]. Relying on this model, Singh[8,9] proposed the formation age of the oldest geomorphic unit, the Varanasi Plain to be ~ 128 ka, representing the last interglacial event, and the age 30–25 ka BP for the formation of the terrace T_1 during the succeeding high sea level stand. The relative dependence of sedimentation rate of the alluvium on neotectonic and climatic events (sea level changes) has still remained unresolved owing to the absence of any reliable dating framework. The only attempt so far to directly date these terraces has been the radiocarbon dating of carbonate nodules embedded in the terrace sediments, which range from 9 to 40 ka (ref. 10). However, radiocarbon ages of the carbonates are often suspect due to contamination either from the modern carbon or the dead carbon[11]. Therefore, in the present paper we examine the feasibility of dating the terrace deposits by the recently developed dating techniques, viz. the thermoluminescence (TL) and infrared stimulated luminescence (IRSL) dating methods. The basic advantage of these methods is that they utilize the minerals constituting the sediment for estimation of the depositional event.

Table 1. Summary of Quaternary lithostratigraphy of the Ganga plain

Age	Lithostratigraphic units including thickness in metres	Lithology and distribution
	New alluvium	
Holocene	Recent alluvium 5–10 m	Confined to present bank limits of the present day rivers comprising bar sand and occasional silt cover.
	Terrace alluvium 10–30 m	Occurring in the terraced valley zones of the present rivers. Comprises alternate sequence of silt and sand.
	Fan alluvium 5–15 m	Coarser clastics with pebbles of all sizes in a radiating channel pattern near the Siwalik Foot Hill.
	Older alluvium	
Lower to upper Pleistocene	Varanasi alluvium > 600 m	Polycyclic sequence of oxidized silt-clay and micaceous sand with ferruginous nodules and kankar disseminations. Covering most part to the north of Ganga–Yamuna axis from Ghaziabad to Ballia. Derived from Himalaya.
	Banda alluvium 120–300 m	Comprises a sequence of silt clay and red quartzo-feldspathic sand with occasional kankar. Covering parts of Bundelkhand and Baghelkhand regions to the south of Ganga–Yamuna developed by peninsular shield.

Luminescence dating is radiation microdosimetry of natural radiation environment. All sediments contain radionuclides, viz. ^{238}U (in ppm), ^{232}Th (in ppm) and ^{40}K (in %). The radiations arising from the decay of these radionuclides along with the cosmic rays provide a constant source of natural radiation flux. The interaction of these radiations with crystal lattice of mineral generates an avalanche of electron and holes. During their motion in crystal lattice, a small fraction of these charges gets trapped at lattice defect sites. The binding energy of the trapped charges at some of these sites is sufficiently high to permit a residence time of trapped charges extending to 10^6–10^8 a at room temperature. This implies that the total number of trapped charges increase with time until a thermal/optical stimulus provides sufficient energy for their detrapping. A small fraction of the detrapped charges radiatively recombine to produce luminescence which bears a proportional relationship to the total radiation exposure. The evaluation of sediment age (t) by TL/IRSL involves measurement of the environmental dose rate (R) and the total dose deposited in mineral (Q). The total dose that accumulated in the mineral grain in the form of total trapped charge concentration is deciphered by measuring the natural luminescence and calibrating it with the luminescence sensitivity of the sample (i.e. luminescence/unit dose). The age is then calculated by dividing the estimated dose (Q) with the environmental dose rate (R).

$$\text{Age } (t) = \frac{\text{Total luminescence}}{(\text{Luminescence/unit dose}) \times (\text{Dose/year})}$$

$$= \frac{Q}{R}. \qquad (1)$$

In the case of sediments, the event dated by luminescence method is the most recent episode of sunbleaching. It is considered that during the predepositional weathering and transport, the minerals are exposed to the sunlight and this exposure causes a photobleaching of 'geological luminescence' to a near 'zero' residual value I_0. The geological luminescence reflects the signal acquired by the mineral during the geological antiquity. On sedimentation and consequent burial, the sun exposure ceases and a fresh accumulation of luminescence (over and above the residual level) I_0 is initiated because of the irradiation from ambient radioactivity. The total luminescence level I_{nat} is related to the luminescence level (I_d) acquired since sedimentation through the relation

$$I_{nat} = I_0 + I_d \qquad (2)$$

and the luminescence age of depositional event is given by

$$\text{Age} = \frac{D(I_d)}{R}, \qquad (3)$$

where $D(I_d)$ is the equivalent laboratory radiation dose required to generate the signal I_d in the bleached sample. An important aspect of application of the luminescence dating is to ascertain the extent of photobleaching by predepositional sunbleaching. For sediment transported in air through suspension or by saltation, the duration of transport and the availability of un-attenuated daylight flux ensures that maximum possible bleaching of the luminescence to a residual value I_0 occurs. On the other hand, sediments transported fluvially, receive an attenuated solar flux due to turbulence in the water and the sediment load[12–14] (see Figure 1). Thus, additional experiments are needed to ascertain the level of photobleaching. These include laboratory bleaching studies using filtered sunlight[15,16] and study of sediments recently deposited under a depositional environment identical to that of the sample[12]. A more recent approach has been to conduct single grain analysis to identify the most bleached mineral grains in a complex suite of samples with grains of different daylight exposure history[17].

Because Indo-Gangetic alluvium sediments are also fluvially transported, two types of experiments, viz. the infrared stimulated luminescence (IRSL) dating and the partial bleach thermoluminescence (TL) analysis were performed. In the IRSL technique, a stimulation with 880 nm source was used. This excitation probes the most sensitive optically stimulable signal[18]. Figure 2 shows the bleaching rate of IRSL of a 90–150 μm K-feldspar mineral separated from the Gangetic alluvium sample on sunlight exposure. It is seen that sunlight exposure can erase 90% of the infrared stimulable signal in few tens of seconds.

Samples for the present study were collected by B. K. Bisaria from different geomorphic surfaces from Budaun,

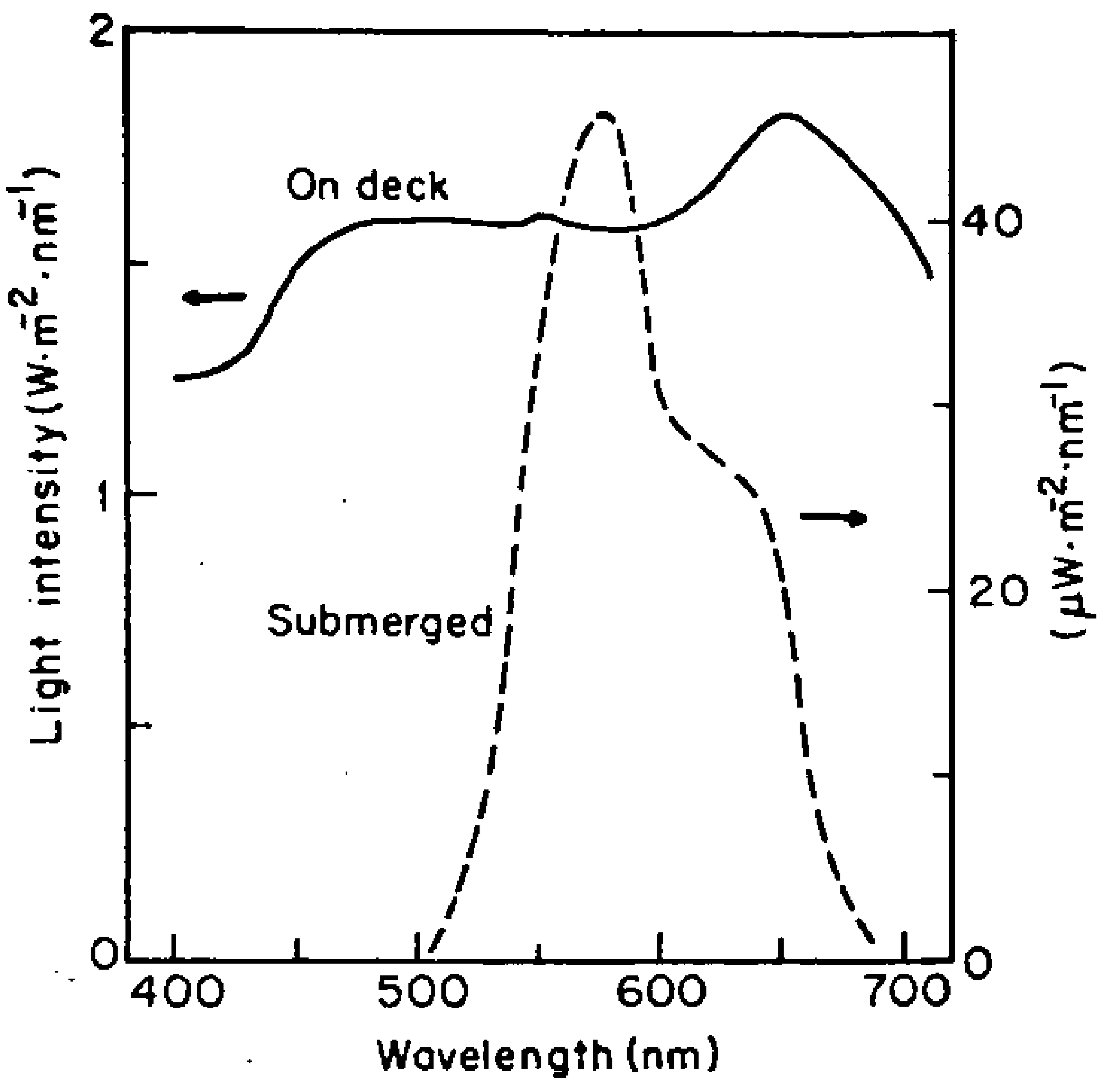

Figure 1. Comparison of sunlight spectrum on deck and at 4 m depth in a turbid river. The intensity at 4 m depth is ~ 10^4 times less than that at the surface. Note also the spectral attenuation below 500 nm and above 690 nm (from Berger and Lutemauer[15]).

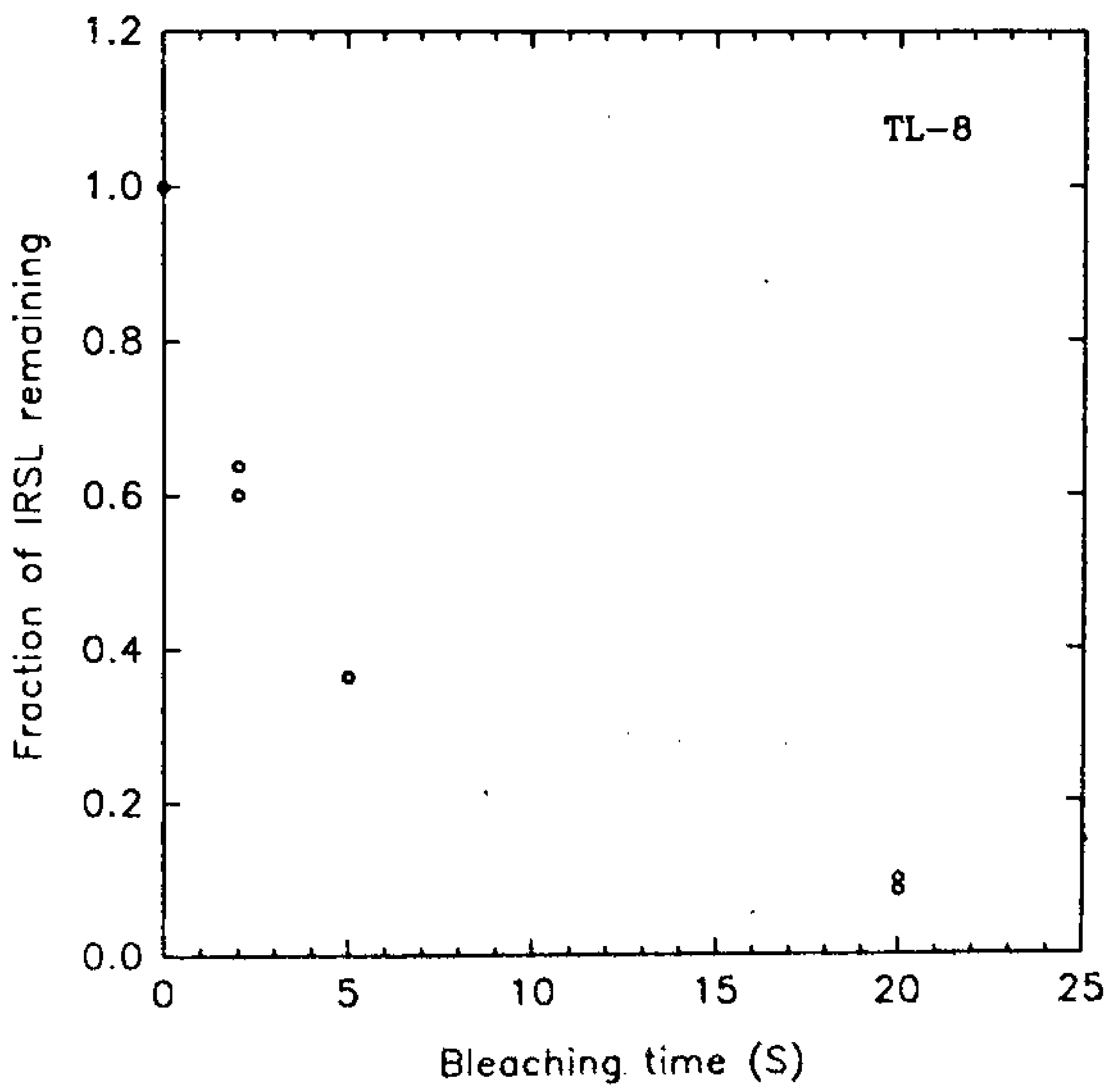

Figure 2. Bleaching of IRSL with sun exposure, expressed as fraction of IRSL remaining for the sample TL-8.

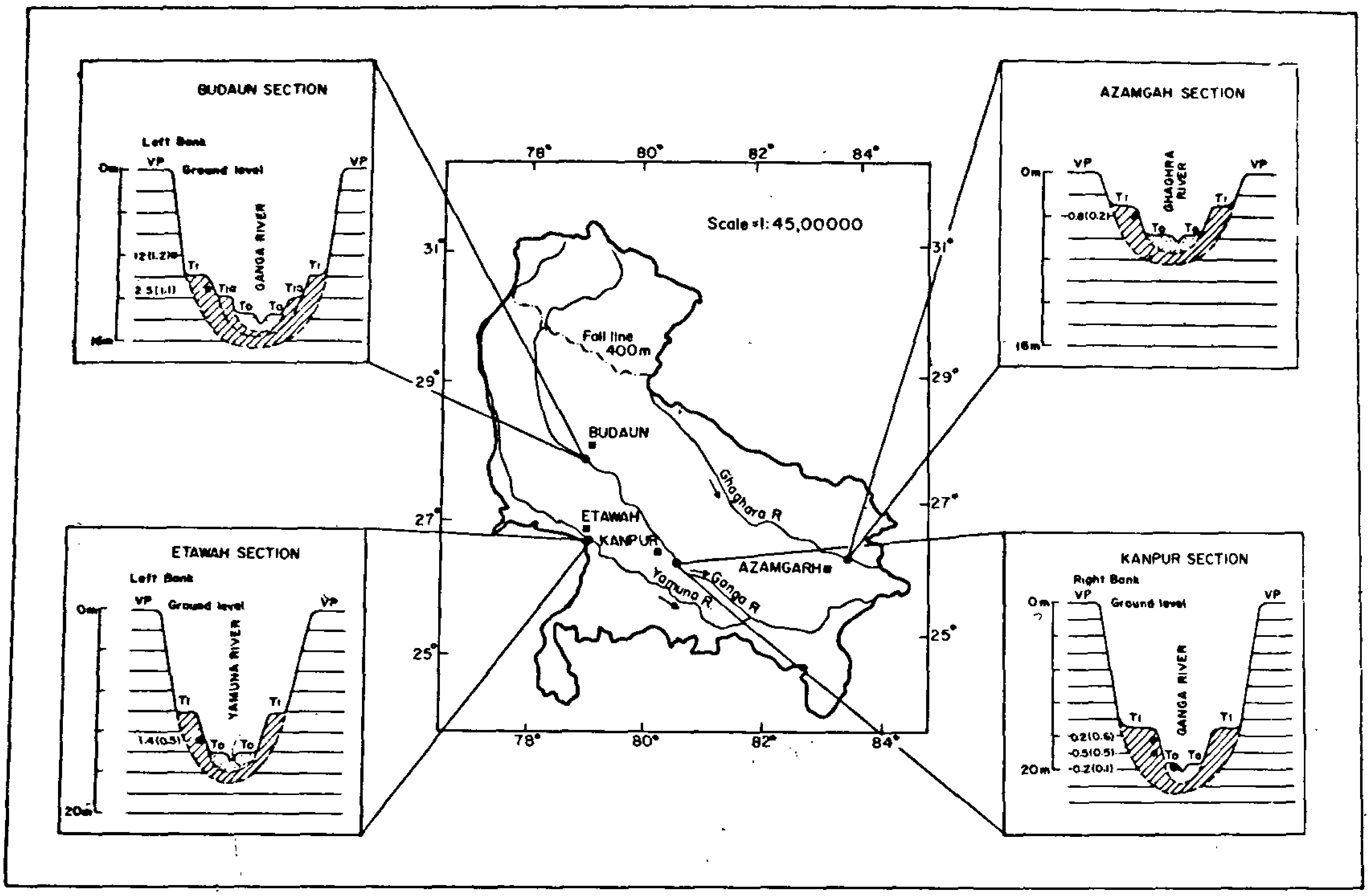

Figure 3. Location of sampling sites, stratigraphic position of sample and IRSL ages.

Table 2. Sample, stratigraphic position, dosimetry data, equivalent dose and luminescence age estimates of samples from Indo-Gangetic alluvium

Sample				Radioactivity data			Dose rate (Gy/ka)			Equivalent dose		Age (ka)	
Code	Site	Terrace	Depth (mbas)	Th (µg/g)	U (µg/g)	K (%)	Internal*	External†	Total dose	TL (Gy)	IRSL (Gy)	TL	IRSL
TL-8	Budaun (North)	T_2	8.0	5.5(1.1)	1.6(0.3)	2.37	0.19	2.86	3.0(0.3)	58(11)	36.5(0.8)	19.0(4.0)	12.0(1.2)
TL-6	Budaun (North)	T_1	11.4	4.7(1.5)	2.1(0.4)	1.08	0.09	2.21	2.3(0.2)	12(16)	5.8(3.0)	5.2(5.8)	2.5(1.1)
TL-34	Etawah (North)	T_1	12.9	14.5(4.6)	3.1(1.1)	1.67	0.13	4.00	4.1(0.3)	14(3)	5.7(2.5)	3.4(0.7)	1.4(0.5)
TL-5	Azamgarh	T_1	4.0	7.1(1.6)	1.8(0.5)	2.40	0.19	3.44	3.6(0.3)	1.5(3)	3.0(0.8)	0.4(0.7)	0.8(0.2)
5/92	Kanpur (R.Bank)	T_1	16.4	13.8(3.9)	2.8(1.2)	1.24	0.10	3.49	3.6(0.2)		0.58(2.9)		0.2(0.6)
6/92	Kanpur (R.Bank)	T_1	18.0	6.1(1.4)	1.9(0.4)	1.11	0.09	2.30	2.4(0.2)		1.3(1.5)		0.5(0.5)
4/92	Kanpur (R. Bank)	T_0	19.7	7.1(2.5)	2.1(0.7)	1.3	0.10	2.63	2.7(0.2)		0.55(0.4)		0.2(0.1)

* For unetched grains external alpha dose estimated by assuming a value as 0.2 ± 0.1.
Cosmic ray dose assumed as 150 µGy/a.
Average 10% moisture content assumed for correcting dose attenuation.
† Internal dose rate estimated by assuming K content as 10%.
The numbers in the parenthesis provide error in the measurement. Thus, 12.0(1.2) is 12.0 ± 1.2.

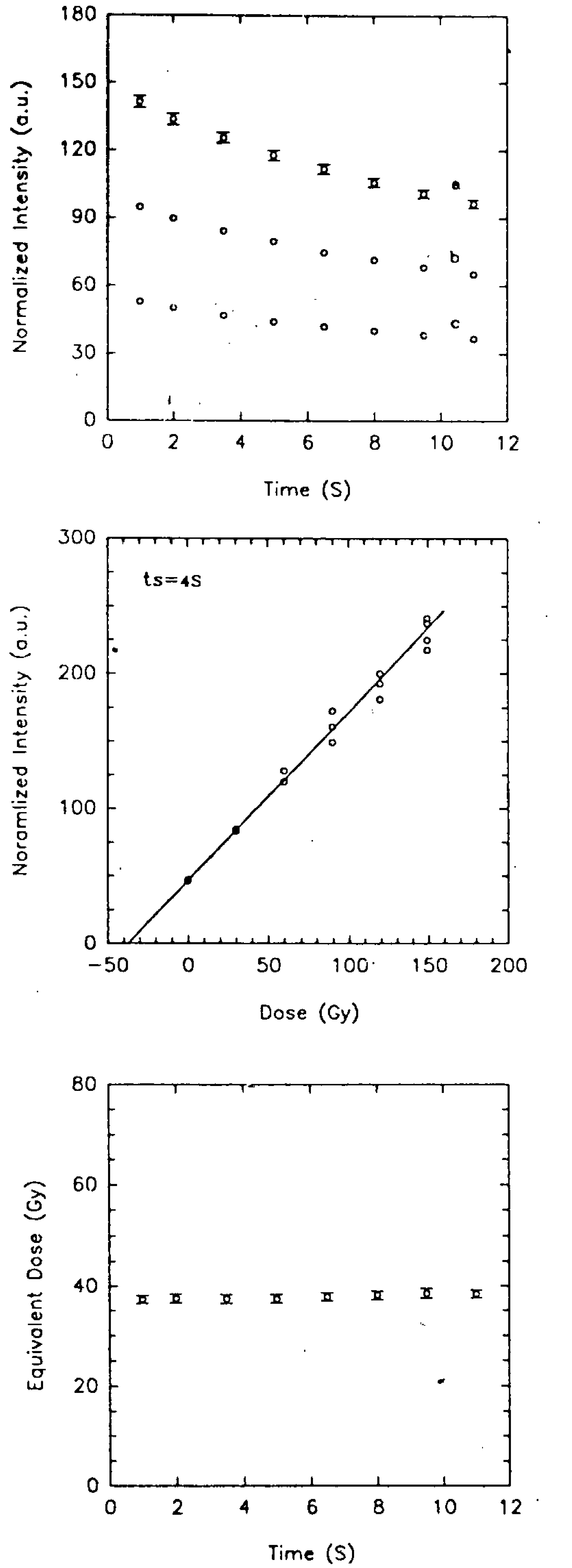

gure 4. Typical IRSL shine curves, growth curves and equivalent ›se plateau for K-feldspar mineral separates for sample TL8. The :SL shine curves are for (a) natural + β-dose (60 Gy), (b) natu-l + β-dose (30 Gy) and (c) natural aliquot.

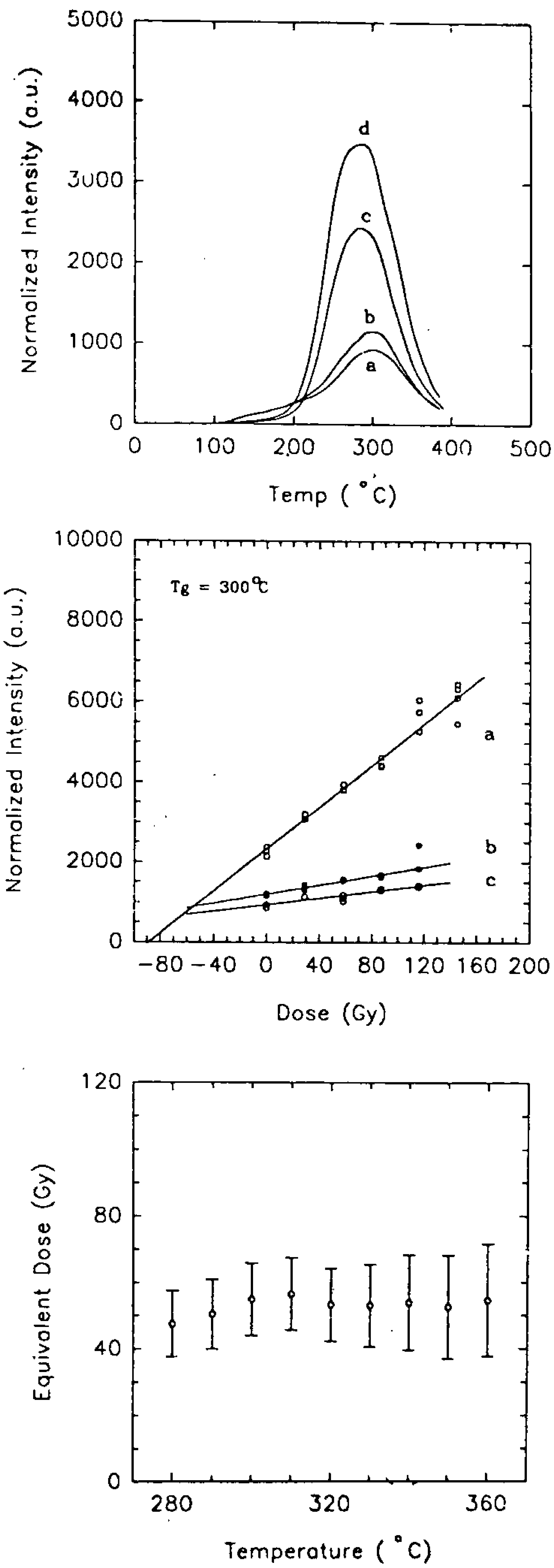

Figure 5. Plot of typical glow curve (top box), growth curve (middle box) and the equivalent dose plateau (bottom box) for K-feldspar mineral separate for sample TL8. The glow curves are for (a) natural + sun bleach (10 min), (b) natural + sun bleach (5 min) and (c) natural aliquot and (d) natural + 30 Gy beta dose. The partial bleach growth curves are for (a) natural + sun bleach (5 min) and (b) natural + sun bleach (10 min). The equivalent dose plateau is for 5 min sun bleach.

Kanpur and Etawa sites in the central region of the Indo-Gangetic plain. Figure 3 shows the sampling localities and the cross-sections of fluvial deposits. The samples were collected as horizontal cores in metal cylinders from freshly exposed vertical cuts. The samples were pre-treated with 1N HCl and 30% H_2O_2 to remove carbonate and organics. The sediment grains of size 90–150 μm were then separated by dry sieving. Feldspar was isolated by density separation (< 2.58 g/cm^3) using a sodium polytungstate compound. Due to the limited sample availability, HF etching of the alpha-exposed layer of these samples, except for BKB-8, could not be attempted. Several monolayer aliquots were obtained from the sample by sprinkling the extracted feldspars onto stainless steel discs, containing silkospray for adhesion.

Irradiations were performed using beta source $^{90}Sr/^{90}Y$ of strength 30 mCi with dose rate of ~0.05 Gy/s. Luminescence from grains was observed using Corning 5-58+7-59 blue transmitting filters combined to an EMI 9635 QA PMT photomultiplier and a photon counting system. For infrared stimulation, an indigenous semi-automated system employing a source made by an array of 16 TEMT 484 diodes, emitting at 880 ± 80 nm was used. The luminescence output from the individual discs was normalized using integrated luminescence obtained from the natural samples on short infrared stimulation for 1 s. Prior to the measurements, the samples were pre-heated for 160°C for 330 min to remove the unstable luminescence signal that is additionally generated during the laboratory irradiation and bleaching procedures. In the analysis, the samples were measured for IRSL for 15 s and then for their TL. This was done on the basis of IRSL stimulation causing an insignificant (~< 2%) depletion of TL signal[19]. In the analysis, the luminescence intensity vs radiation dose growth curves were fitted to linear regressions. In estimating the dose rate, uranium and thorium concentrations were measured using thick source alpha counting and potassium was estimated by atomic absorption spectroscopy. The concentrations were converted into dose rates using conversion table provided in Aitken[20] (assuming the decay series to be in radioactive equilibrium). An average 10% water content and 150 μGy/a cosmic ray dose was assumed in calculating the dose rates. The internal β-dose has been calculated using the factor provided by Mejdahl[21] and assuming a 10% internal potassium content. For the unetched samples, the alpha-dose has been estimated assuming an alpha efficiency of 0.2 ± 0.1 (ref. 22). The error in age was estimated using the prescription of Aitken[20].

Table 2 provides a summary of TL and IRSL data and Figures 4 and 5 provide typical shine down curve, growth curve and plateaux for IRSL and glow curve, growth curve and plateaux for TL data. Both the TL and IRSL ages show a stratigraphic consistency. These ages are also concordant with the previous TL age estimates on similar terrace sequences from Roorkee area[12]. Note that the age 200 years obtained on surface sediment suggests that the luminescence signal is definitely bleached prior to burial and this age also can be taken as the lower limit to the ages obtainable by the IRSL technique. The age 200 years for surface samples can also be considered as the over-estimation amount for all the samples deposited under similar conditions. From Table 2 it is apparent that TL ages are somewhat higher compared to their IRSL ages. In view of easy bleachability of IRSL and the near zero IRSL age of the surface sample, we consider IRSL ages to be more realistic compared to the corresponding TL ages. The age of the Varanasi Plain at Budaun site is obtained as 12 ka is consistent with the radiocarbon age of ~12 ka obtained at this depth deduced from the data from Kanpur and Fatehpur sequences (Figure 2 of Rajgopalan[10]). The ages on terrace T_1 suggest their formation during late Holocene period. The low TL/IRSL ages on T_1 and Varanasi Plain suggest either that these terraces are substantially younger than the inferred age[8,9], or that they are part of the Holocene aggradation deposits. The ages arrived at for Varanasi Plain and T_1 terraces are in concordance with evolutionary model of the Ganga Plain as suggested by Bisaria *et al.*[7]. More detailed chronological work is needed to conclude the age bracket for these terraces.

The preliminary dating results show that the zeroing of luminescence signal indeed occurred for these samples and that the ages are stratigraphically consistent, demonstrating the reliability of the technique and its future prospects in examining the time evolution of the Indo-Gangetic sequence.

1. Pascoe, E. H., *A Manual of the Geology of India and Burma*, Govt. India Publ., Delhi, 1973, vol. III, pp. 1346–2130.
2. Rao, M. B. R., *J. Geol. Soc. India*, 1973, **14**, 217–242.
3. Khan, E. A., Pandey, B. N. and Bisaria, B. K., *GSI Rec.*, 1989, **122**, 91–94.
4. Pandey, B. N., Bisaria, B. K. and Srivastava, A. B., *GSI Rec.*, 1992, **125**, 37–40.
5. Pandey, B. N. and Bisaria, B. K., *GSI Rec.*, 1994, **127**, 173–175
6. Sastri, V. V., Bhandari, L. L., Raju, A. T. R. and Dutta, A. K., *J. Geol. Soc. India*, 1971, **12**, 222–233.
7. Bisaria, B. K., Pandey, B. N., Khan, A. U. and Bhartiya, S. P., Abstracts: Symposium on Recent Advances in Geological Studies of NW Himalaya and Foredeep, GSI, Lucknow, Feb. 21–23, 1995.
8. Singh, I. B., in *Gangetic Plain: Terra Incognita* (ed. Singh, I. B.), Geol. Dept, Lucknow University, 1992, pp. 1–14.
9. Singh, I. B., *Indian J. Earth Sci.*, 1987, **14**, 272–282.
10. Rajgopalan, G., in *Gangetic Plain: Terra Incognita* (ed. Singh, I. B.), Geol. Dept, Lucknow University, 1992, pp. 45–48.
11. Lallen, R. A., Wasson, R. J. and Gallispie, R., *Sediment. Geol.*, 1992, **35**, 1–4.
12. Vohra, S., M Tech thesis, University of Roorkee, Roorkee, 1987.
13. Gammell, A. M. D., *Quat. Sci. Rev.*, 1988, **7**, 339–345.
14. Berger, G. W., *J. Geophys. Res.*, 1990, **B95**, 12375–12397.
15. Berger, G. W. and Luternauer, *Geol. Surv. Canada*, 1987, **87-1A**, 901–904.

16. Fuller, I. C., Wintle, A. G. and Duller, G. A. T., *Quat. Geochron. (Quat. Sci. Rev.)*, 1994, **13**, 539–543.
17. Lamothe, M., Balescu, S. and Auclair, M., *Radiat. Meas.*, 1994, **23**, 555–561.
18. Hutt, G., Jaek, I. and Tchonka, *Quat. Sci. Rev.*, 1988, 7, 381–385.
19. Botter-Jensen, L., Ditlesen, C. and Mejdahl, V., *Nucl. Tracks Radiat. Meas.*, 1991, **18**, 257–263.
20. Aitken, M. J., *Thermoluminescence Dating*, Academic Press, New York, 1985, p.359.
21. Mejdahl, V., *Archaeometry*, 1979, **21**, 61–73.

ACKNOWLEDGEMENTS. We thank Shri Ravi Shanker, Geological Survey of India, Lucknow and Shri Gopendra Kumar, Director (Retd.) for their help with the sample collections and for their keen interest.

Received 3 October 1996; revised accepted 25 February 1997

Record of the Cretaceous magnetic quiet zone: A precursor to the understanding of evolutionary history of the Bay of Bengal

M. V. Ramana, V. Subrahmanyam, K. V. L. N. S. Sarma, Maria Desa, M. M. Malleswara Rao* and C. Subrahmanyam[†]

National Institute of Oceanography, Dona Paula, Goa 403 004, India
*National Institute of Oceanography, Regional Centre, 157 Lawsons Bay Colony, Visakhapatnam 530 016, India
[†]National Geophysical Research Institute, Hyderabad 500 007, India

Magnetic study along a transect joining the sites of Ocean Drilling Programme (ODP) leg 116 (1°S, 81°24′E) and the vicinity of Deep Sea Drilling Project (DSDP) site 218 (7°N, 87°30′E) revealed the presence of a wide magnetic smooth zone sandwiched between the known Late Cretaceous anomaly A34 (≈ 84 Myr) and the younger magnetic anomaly sequence of Early Cretaceous crust, represented by M0 (≈ 118 Myr). The smooth magnetic zone seems to have evolved during the Cretaceous long normal polarity epoch (superchron K–T) 118–84 Ma and is usually referred to as the Cretaceous magnetic quiet zone. Identification of this zone in the distal Bengal Fan perhaps serves as a missing link between the Early Cretaceous and the Late Cretaceous evolution of the crust and establishes a continuous evolutionary record of the Bay of Bengal since India's breakup from the eastern Gondwanaland continents.

SEVERAL plate reconstruction models have been proposed for the breakup of Pangea and the eastern Gondwanaland, in which the east coast of India and the Enderby Landmass of Antarctica were juxtaposed and the western margin of Australia lies east of Greater India during the Late Jurassic[1–11]. The breakup of India from the Antarctica–Australian plate sets the stage for the evolution of the Bay of Bengal and the eastern Indian Ocean. The Bengal Fan is one of the thickest sedimentary basins of the world[12–15]. Powell *et al.*[7] were of the view that the magnetic anomalies will be hard to find off the east coast of India due to huge sediment accumulation. Though extensive underway geophysical data was collected during the International Indian Ocean Expedition Programme (1959–1965) and subsequent expeditions to unravel the evolutionary history of the Indian Ocean[16–19], not much was known about the age and nature of the ocean floor of the Bengal Fan[6,7,20,21]. Various plate reconstruction models[5,7,22] show the stage-by-stage evolution of the eastern Indian Ocean since the Late Cretaceous (84 Myr) to the Present. However, refined plate reconstruction models for the early opening prior to Late Cretaceous are poorly constrained[10] due to inadequate geophysical data, particularly in the Bay of Bengal, northeastern Indian Ocean.

Recent geophysical studies[23,24] in the northern Bay of Bengal revealed the presence of N30°E trending Mesozoic magnetic anomaly sequence M11 to M0 (corresponding 132.5 to 118 Myr age old crust) and N120°E (≈ NW–SE) trending fracture zones (Figure 1). The direction of these fracture zones indicates the initial motion of the Indian plate from Antarctica–Australia immediately after the Early Cretaceous breakup. In the present study, a smooth magnetic field has been observed on a transect joining the sites of ODP leg 116 and the vicinity of DSDP site 218 over a distance of about 415 km continuing from the known Late Cretaceous anomaly A34 (≈ 84 Myr) and culminating with the Early Cretaceous crust. This magnetic smooth zone is significant for establishing the continuous evolutionary history of the Bay of Bengal since India's separation from the eastern Gondwanaland during the Early Cretaceous.

About 1200 line km of bathymetry, magnetic, gravity and multichannel seismic reflection data along the transect joining the sites of ODP leg 116 and the vicinity of DSDP site 218 have been collected onboard *ORV Sagarkanya* during 1995 (April–May). The processed data (Figure 2) has been used to infer the nature and age of the crust in the distal Bengal Fan to better constrain the evolutionary history of Bengal Fan.

The identification of the Early Cretaceous crust[23,24] and the Late Cretaceous crust[5,22] in the northern and southern Bay of Bengal respectively suggests that the ocean floor of the Bay of Bengal should have a continuous evolution record since the Early Cretaceous. This can be established either by the sampling of the oceanic basement rocks or by the study of seafloor spreading type of magnetic anomalies. We have used the total intensity earth's magnetic field data to infer the nature of the basement. The observed magnetic